223, 233 (1989).
11. V. I. Moruzzi, J. F. Janak, and A. R. Williams, "Calculated electronic properties of metals", p. 148, Pergamon Press Co., New York, U.S.A., 1978.
12. F. Hultén and I. Persson, *Acta Chem. Scand., Ser. A* 401 (1987).
13. K. A. Jøgensen and R. Hoffmann, *J. Phys. Chem.*, **94**, 3046 (1990).
14. J. E. Demuth and P. N. Sanda, *Phys. Rev. Lett.*, **47**, 57 (1981).
15. R. M. Hochstrasser and C. Marzzacco, *J. Chem. Phys.*, **49**, 971 (1968).
16. J. Sadlej and I. L. Cooper, "Semi-empirical methods of quantum chemistry", p. 293, John Wiley & Sons, 19 85.
17. J. T. Golab, J. R. Sprague, K. T. Carron, G. C. Schatz, and R. P. Van Duyne, *J. Chem. Phys.*, **88**, 7942 (1988).
18. B. H. Loo, *J. Electronal. Chem.*, **131**, 381 (1982).
19. X. Jiang and A. Campion, *Chem. Phys. Lett.*, **140**, 95 (1987).
20. J. A. Creighton, *Surf. Sci.*, **173**, 665 (1986).
21. T. N. Rhodin and G. Ertl, "The Nature of the Surface Chemical Bond", p. 63, North-Holland., 1984.

Micellization of Dodecyltrimethylammonium Bromide in D_2O as Probed by Proton Longitudinal Magnetic Relaxation and Chemical Shift Measurements

Yoon Seob Lee and Kyu Whan Woo*

Department of Chemistry Education, Seoul National University, Seoul 151-742
Received February 19, 1993

^{1}H-NMR chemical shifts and relaxation rates of dodecyltrimethylammonium bromide (DTAB) were measured in aqueous solutions as a function of solute concentrations. Downfield chemical shifts were found on micellization for all protons. Critical micelle concentration (CMC), aggregation number (n), equilibrium constant (K) and chemical shifts of monomer and micelle (δ_{mono}, δ_{mic}) were obtained from chemical shifts measurement. In spherical DTAB micelle which is confirmed by the calculated value of surface area, the hydrocarbon chain had two gauche connections in opposite directions in average. When micelles were formed the relaxation rates of all protons were greatly increased, as their environment changed from water to liquid hydrocarbon. The variation of relaxation rates indicate that 1) part of the surfactants molecules in the micelles, *i.e.*, the head groups, are exposed to the water, 2) molecular motion in the micellar state is more resticted than in monomer state and 3) the penetration of the water molecules into micelle interior reach to the α position. A deformation from spherical to ellipsoidal micelles has been suggested for DTAB when the surfactant concentration is higher than 32.0 mM. An explanation of this possibility is given.

Introduction

Amphipathic molecules those possessing clearly defined regions of both hydrophobic and hydrophilic character are well known to form a variety of structures in an aqueous environment in which the hydrophilic moiety is exposed to the solvent and the hydrophobic one is hidden from it. These include spherical micelles, ellipsoidal micelles, rod-shaped micelles, and a variety of smectic mesophases including bilayers, vesicles, liposomes, and lamellaphase. Micelle formations of a surfactants in solution is induced by the hydrophobic interaction between hydrocarbon parts of the surfactant molecules balanced by their hydration and electrostatic repulsive effects. A micelle is formed cooperatively at CMC[1], which is characteristic of the surfactant species and that CMC is usually influenced by various factors such as temperature and ionic strength. If the length of the hydrophobic chain is increased, the hydrophobic effect becomes more strong and, consequently, the CMC decreases and larger micelles are formed.[2,3] Such micelle structures derived from simple surfactant molecules serve as both structural and functional models for more complex ones, including proteins and biomembranes, constructed from the correspondingly more complex biological surfactants, particularly phospholipids and cholesterol.[4]

DTAB[1] is one of the cationic surfactant which has been extensively studied by physicochemical methods. Aqueous DTAB solutions show a considerable complexity in many properties and, in particular its rather high CMC (15.0-16.0 mM)[5-7] and sufficiently long alkyl chain length is suitable to the studies of common characters of various micelles. It is evident that the origin of the complexity of DTAB solutions, as it is expressed in the various physicochemical properties, has to be sought in various structural changes of the aggregates formed. In turn, aggregated shapes and aggregation process have to be traced back to the different types of interactions at the molecular level, *i.e.*, surfactant-surfactant, surfactant-water, surfactant-courterion, surfactant-solubilisate, etc. In order to study the highly specific effect on aggregate structures and processes in aqueous DTAB so-

lutions further, and in particular of elucidating the underlying molecular interactions, we have undertaken nuclear magnetic resonance investigations.

In aqueous media, the micellization of ionic surfactants are greatly influenced by both main alkyl chain and counterion species in the solution. A change from spherical to rodlike micelles has been mainly suggested till now when the concentration of surfactant or added salt exceeds a certain critical value. In the case of DTAB this change occurs in the absence of added salt when the concentration of DTAB is larger than about 700 mM[8], which is much higher than the critical micelle concentration. However, the concentration range between the above two is so wide that another deformation of spherical micelle shape into ellipsoidal one which makes the sphere-to-rod transition smooth has been suspected in this concentration range. In recent work, this possibility was proposed strongly by calculation based upon the SCFA (self-consistent field lattice theory for adsorption or association of chain molecules) theory.[9] Proton NMR relaxation measurements on micellar system can be used to separate the contributions from rotational and translational motions to the relaxation process, and yield information about differences in the degree of mobility along the hydrocarbon chain.

In the present study the size of spherical DTAB micelle and the possibility of the above deformation in aqueous solution are investigated through the measurements of the proton NMR chemical shift and spin-lattice relaxation rate.

Experimental

DTAB was purchased from Aldrich-Chemie, West-Germany and used as supplied without further purification. It was dried *in vacuo* at room temperature for at least 3 days before use. As a check of the purity of the surfactant CMC determination was performed; the CMC agreed closely with those of others.[5-7] Deuterium oxide was supplied by Sigma Chemical Co., USA and was 99.9% enrichment. All surfatant solutions were prepared by weighing, and the concentrations are given as mM (milimoles/L of D_2O).

Proton NMR investigations were performed on a Hitachi R-600 high resolution NMR spectrometer in the Fourier-Transform mode. The deuterium signal from D_2O was employed as an internal lock signal. The experiments were performed at a fixed temperature (34.2℃) which is calibrated from the chemical shift difference between the two proton resonance of standard MeOH sample.[10] The oxygen was removed by repeated, at least 5 times, freeze-pump-thaw cycles, and the tubes were sealed under vacuum condition. No susceptibility corrections have been applied. In measurement of chemical shift, the residual HOD proton resonance ($\delta=5.14$ ppm) served as an internal reference. The spin-lattice relaxation time T_1 was measured by the ordinary 180°-τ-90° pulse sequences. The precision of the T_1 measurements of our sample was better than ±3%.

Results and Discussion

Micelle size. In the pseudophase model of micelle formation, the CMC is considered as a transition point between the monomeric and aggregated states of the surfactant. If

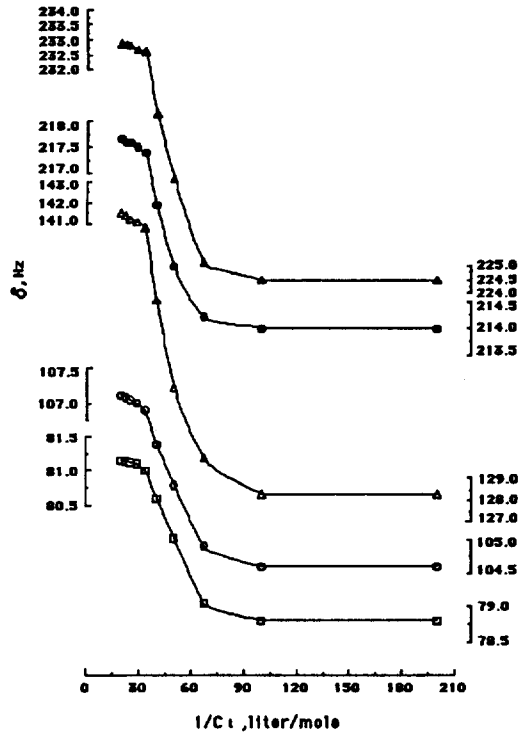

Figure 1. Plot of chemical shifts of various protons of DTAB as a function of reciprocal surfactant (DTAB) concentration in water (D_2O). The vertical axis have break, because the different chemical shifts corresponding to different segments in the surfactant molecule. (● : N, ▲ : α, △ : β, ○ : m, □ : ω).

the exchange rate of surfactant molecules between the aqueous bulk solution and the micelle is fast compared to the chemical shift difference (δ_{mic}-δ_{mono}) between the free monomer and the aggregate, the observed shift of a resonance line is a weighted average of their contributions. Therefore, the observed chemical shift, δ_{obs}, is

$$\delta_{obs}=\delta_{mono}\cdot\frac{C_{mono}}{C_t}+\delta_{mic}\cdot\frac{C_{mic}}{C_t} \quad (1)$$

As a consequence of basic assumption there is no aggregation below the CMC whereas the monomer concentration, C_{mono}, above the CMC remains constant. Inserting $C_{mic}=C_t-\text{CMC}$ into Eq. (1) where C_{mic} and C_t is the micelle and the total surfactant concentration, respectively, we obtain a linear function of δ_{obs} *vs.* the inverse of the total concentration.

$$\delta_{obs}=\delta_{mic}-\frac{\text{CMC}}{C_t}\cdot(\delta_{mic}-\delta_{mono}) \quad (2)$$

The plot of δ_{obs} against $1/C_t$ in spherical micelle region yield δ_{mono}, δ_{mic} and the CMC.[11-14]

In Figure 1, the ^1H chemical shifts of DTAB in water are plotted against reciprocal of the total concentration. The notation used to describe the various protons of surfactant segments are as follows:

$$\underset{(CH_3)_3}{\overset{+}{N}}\text{-}\underset{\alpha}{CH_2}\text{-}\underset{\beta}{CH_2}\text{-}\underset{m}{(CH_2)_9}\text{-}\underset{\omega}{CH_3}$$

δ_{mono}, δ_{mic} and CMC of DTAB micelle were determined from the two straight lines drawn at high and low surfactant con-

Table 1. Several Micelle Parameters of DTAB deduced from Chemical-Shift Measurements of the Protons of DTAB in Water (D_2O)

Parameter / Position	1st. CMC	δ_{mono}	δ_{mic}	Δ	n	$\ln K$
	mM		Hz			
N	15.3	214.0	220.5	6.5	35.6	139.6
α	15.2	224.5	240.2	15.7	35.9	140.8
β	15.3	128.3	152.4	24.1	35.9	140.2
m	15.3	104.6	109.2	4.6	36.4	144.8
ω	15.2	78.8	83.2	4.4	35.1	139.7
average	15.3				35.8	141.0

centration (region above 30 liter/mole). Figure 1 clearly indicates that the resonance signals of all protons undergo significant downfield shifts upon micellization.

Regarding the orgin of the chemical shift changes on micelle formation we can visualize two principal mechanisms. We may either have 'medium effects', *i.e.*, direct effects of the environment, or we may have 'conformation effects', *i.e.*, the chemical shift may change as a result of a change in conformation of the hydrocarbon chain.[2] Since a downfield shift can be related to an increasing importance of the *trans* conformation,[2,16] it can be inferred from Figure 1 that micelle formation is accompanied by conformational change from gauche to *trans* in the part of hydrocarbon chains. It is significant that the effects are large to the α direction while relatively small to the ω end. Several observations[2,16] show that the medium effect of water on the polar head is remarkable. Upon micellization, due to the binding of the counterion (Br^-) on micellar surface the water structure is somewhat rigidified.

In Figure 1 and Table 1, it is shown that the order of the change of chemical shift is

$$\beta \gg \alpha \gg N \geq m \cong \omega$$

Therefore it can be infered from the above order that the medium effect of water at the polar head is comparable to the conformation effect at the middle of the hydrocarbon chain.

Ulmius *et al.*[17], also verified the conformation effect in the system of mixed micelles in which 1 : 1 $TTAC^1+CTAB^1$ or $TTAC+CTAC^1$ solutions with a total concentration of 15% by weight. In that case the TTA^+ ω signal moves downfield 0.08 ppm and the CTA^+ ω signal moves upfield with the same amount as compared to the single surfactant solutions.[18] The downfield shift of the TTA^+ ω could be ascribed to a larger proportion of *trans* conformations as mentioned above, because the motions of the ω will be restricted when surrounded by the CTA^+ alkyl chains. Similar restriction of hydrocarbon chain in our case could occur in the micellization of DTAB.

In order to obtain the aggregation number of micelle, we applied the single step equilibrium model (the mass action law of micelle formation) on the micellization of DTAB. Assuming an idealized situation where the amphiphile may occur either as a monomer or a single type of micelle with an aggregation number n the chemical shift can be written

$$\delta_{obs} = \frac{C_{mic}}{C_t} \cdot \delta_{mic},$$

where both δ_{obs} and δ_{mic} are taken relative to the chemical shift of the monomer. The equilibrium between the monomeric and micellar surfactant is given by

$$n A \rightleftharpoons A_n$$

with equilibrium constant

$$K=[A_n]/[A]^n$$

The concentrations of monomer and micelle in the equilibrium may be expressed as

$$[A]=C_t \cdot \frac{\delta_{mic}-\delta_{obs}}{\delta_{mic}} \quad \text{and} \quad n\cdot[A_n]=C_t \cdot \frac{\delta_{obs}}{\delta_{mic}}.$$

The expression for K may then be rewritten as

$$\ln(C_t \cdot \delta_{obs}) = n \cdot \ln[C_t \cdot (\delta_{mic}-\delta_{obs})]+\ln K+\ln n-(n-1)\cdot \ln \delta_{mic} \quad (3)$$

Consequently, a plot of $\ln(C_t \cdot \delta_{obs})$ *vs.* $\ln[C_t \cdot (\delta_{mic}-\delta_{obs})]$ yields the aggregation number and the equilibrium constant. Analogous procedures have been used previously for chemical shift of various nuclei.[19-22] The results are summarized in Table 1. The aggregation number obtained from ^{1}H-NMR chemical shift is 35.8± 0.4. This aggregation number is in close agreement with the theoretical value of 37.1 which is calculated by SCFA theory.[9]

The head group area, a, and hydrocarbon core radii, R_{hc}, have been computed by assuming spherical micelle, with an oil-like hydrocarbon interior, by taking

$$n \cdot v=(4\pi/3)\cdot R_{hc}^3, \quad (4)$$

$$n \cdot a=4\pi \cdot R_{hc}^2. \quad (5)$$

Here v is the known volume of the hydrocarbon tail estimated as v=(27.4+26.9 m) Å^3 where m is some value close to but slightly smaller than the number of carbon atoms per hydrocarbon chain.[23] Using n=35.8 of our results of ^{1}H chemical shift and v=350 Å^3 for the hydrocarbon chain of 12 of X-ray scattering results,[23] we obtained the value of R_{hc}=14.4 Å. Because the fully extended chain length is (l_{max}=1.5+1.265 m) Å by the theory[23], for this surfactants, l_{max}=16.7 Å. Hydrocarbon chain in the interior of micelle can not be expected as fully extended state, so that the effective length of a chain (perpendicular to the micelle surface), which is equal to R_{hc}, is less than l_{max}. In bulk liquid the difference can be estimated based on the statistical mechanics of polymer chain dimensions.[24] In the spherical micelle, each 'kink' illustrated by Tanford[25] would reduce the hydrocarbon chain length by 1.25 Å. And for two kinks per hydrocarbon chain, R_{hc}/l_{max} would be about 0.84 for a typical chain length. From our results, R_{hc}/l_{max}=0.86. Consequently in spherial micelle region of DTAB, the hydrocarbon chains have two gauche connections in opposite directions, creating two kink in average.

For the sake of simplicity, if we assume that the centers of the three methyl groups of the head group of DTAB represent three of the four apexes of a regular tetrahedra with the N^+ at the center of this one, we can calculate the radius

of spherical micelle, R, which include the contribution of head group. The fourth apex would lie on the dodecyl hydrocarbon chain. We assume that the contribution of the nitrogen atom is equal to 1.265 Å. Thus the radius is

$$R=1.6+1.265\cdot(m+1)+0.421\cdot m'$$

where $m'=1$ for the methyl group of head. For the DTAB this radius can be determined as 18.5 Å. Comparing with the l_{max}, it can be infered that the non-permeated head group thickness of spherical micelle is 1.8 Å.[26] Adding this value we obtain a value of 16.2 Å for the micellar radius, somewhat smaller, than the experimental finding with 'a two-step model' from the multifield relaxation data.[27] As mentioned above these come from the difference of the state of hydrocarbon chain the micelle interior. Although it is expected that the form of fully stretched hydrocarbon chain has a minimum free energy, if we consider the lateral diffusion coefficient of DTAB micelle,[28] $D=(4.6\pm0.8)\times10^{-11}m^2\cdot s^{-1}$, we can accept the above difference. Eq. (4) and (5) assume that the density of hydrocarbon is constant in the interor of the micelle.[29] Thus head group area per hydrocarbon chain of $a=72.4$ Å^2 was obtained from Eq. (5) and is good agreement with the bromide specific electrode measurement of Zana.[26]

According to the reference paper,[23] the free energy per amphiphile in a micelle is given by

$$\mu_N^0=\gamma\cdot\left(a+\frac{a_o^2}{a}\right)+g.$$

Where the interfacial free energy per unit area of aggregate, γ, is close to 50 erg $\cdot$ cm^{-2} characteristic of the liquid hydrocarbon-water interface. This value has been shown to be essentially the surface tension of water minus the dispersion energy contribution at the water-hydrocarbon interface. And g the bulk free energy per amphiphile. Henceforth a_o will be referred to as the optimal surface area per amphiphile, being that area at which the free energy per amphiphile in a micelle is a minimum. Since $a_o=(4\pi)^{1/3}\cdot(3v)^{2/3}/n^{1/3}$, and the tail volume of an hydrocarbon chain is known, we can yield the 72.7 Å of a_o, in approximate equal to a. According to another theory[30] which classify the micelle shape in terms of new parameters, we have spherical micelles in case of $v/a_o\cdot l_{max}<1/3$; globular micelles or rods in case of $1/3<v/a_o\cdot l_{max}<1/2$, in which the evolution of shape from globular to rod accompained with this value going to higher value; liposomes, lamella phase in case of $v/a_o\cdot l_{max}>1/2$; reversed phases in case of $v/a_o\cdot l_{max}>1$. Whatever the shape, the tail volume of v and fully stretched chain length of l_{max} (for vesicles the outher chain length) is independent with the evolution of micellar shape. In our works, $v/a_o\cdot l_{max}$ yields 0.288, which consequently support our assumption of spherical DTAB micelle.

When the total concentration of surfactant increases gradually to some extent in spherical micelle region, the spherical micelle begins growing to some larger one not persistent its initial size,[9] so that the area per hydrocabon chain do not satisfies the assumption of $a=a_o$, and almost everywhere above a certain critical surfactant concentration, it begins to decrease. Therefore, it can be expected that the spherical micelle is deformed to another shape above this critical concentration as the value of $v/a_o\cdot l_{max}$ exceeds 1/3. Israelachvili *et al.*, proposed[23] a ellipsoidal forms as this another shape in the globular micelle region by purely mathematical calculation. Thus, we calculate from the $v/a_o\cdot l_{max}$ value of 1/3 that this elliposidal micelle has about 56 of aggregation number above a certain critical surfactant concentration in case of aqueous DTAB soluion.

In Table 1 the value of ln $K=141.0\pm1.9$ was determined in average as the equilibrium constant in the aggregation process of surfactant molecules into spherical micelles. The values of CMC, n, and K obtained from various proton resonances are in excellent agreement.

From Table 1, it is seen that the change of the chemical shifts on micellization $\Delta=\delta_{mic}-\delta_{mono}$ is dependent on the position of the proton along the molecular chain. At the β positon of the molecule the largest downfield shift of 24.1 Hz is observed. The shift becomes progressively small as the position of the proton atom reaches either polar head or chain end. The degree of shielding of a proton atom depends on relative populations of 'gauche' and '*trans*' conformers. Downfield shifts on micellization suggest increased fraction of '*trans*' conformer along the carbon chain where respective protons are attached. The spin-lattice relaxation rates of respective protons discussed later also show the presence of motional gradient along the hydrocarbon chain. Both in Table 1 and Figure 3, we look at the Stern layer of micelle. It is seen that chemical shift of the protons at head position is a little affected on micellization and that its relaxation rate is rather small than that of α, β position. Accordingly, the methyl groups attached to nitrogen atoms are considered to stick out from the surface of a spherical micelle into the solvent and their motional freedom as well as their magnetic environment are not altered significantly on micellization. The same tendency about the changes of conformations of hydrocaron chain on micellization was found in case of DDAC[1] by Maeda *et al.*[31]

The evolution of micelle shape. The contribution of the deuterium of D_2O or bromine nuclei of counterion to the relaxations of DTAB protons is very small and can be ignored. In our systems, therefore it can be assumed that (i) only dipole-dipole interaction between protons in the surfactant molecules is effective in causing spin-lattice relaxation, and (ii) molecular motion is sufficiently rapid that the 'extreme narrowing' condition exists.

In Figure 2, the ^1H spin-lattice relaxation rates at various positions were plotted as a function of the total surfactant concentration in water (D_2O). All the protons showed the similar variation of $1/T_1$ in the beginning, *i.e.*, slightly increased with increasing the DTAB concentration up to 16.0 mM. But above this concentration, the relaxation rates of all protons abruptly increased up to 32.0 mM. After this total concentration, the relaxation rates itself were increased but very gradually as the concentration is increased. The first critical point of 16.0 mM is well known as the 1st. CMC of this surfactant, in good agreement with the result of ^1H chemical shift and the several other experimental[32] and theoretical[9] values.

The $(1/T_1)_{intra}$ (sec^{-1}) of each protons were determined by extrapolation to infinite dilution in Figure 2. The results are as follows:

	N	α	β	m	ω
$(1/T_1)_{intra}$	0.62	0.73	0.97	0.65	0.34

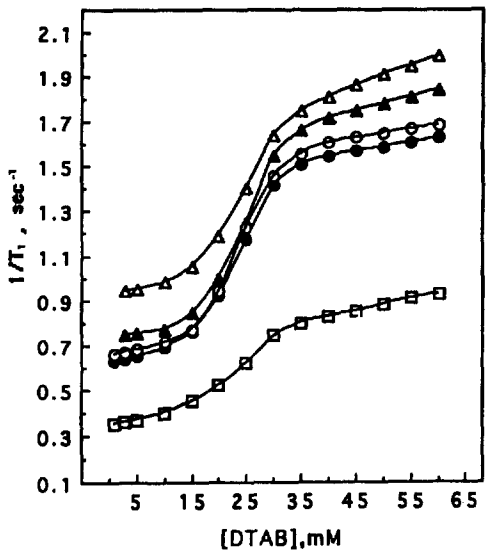

Figure 2. Plot of proton spin-lattice relaxation rate ($1/T_1$) of various protons of DTAB as a function of the concentration of DTAB in water (D_2O). (● : *N*, ▲ : α, △ : β, ○ : *m*, □ : ω).

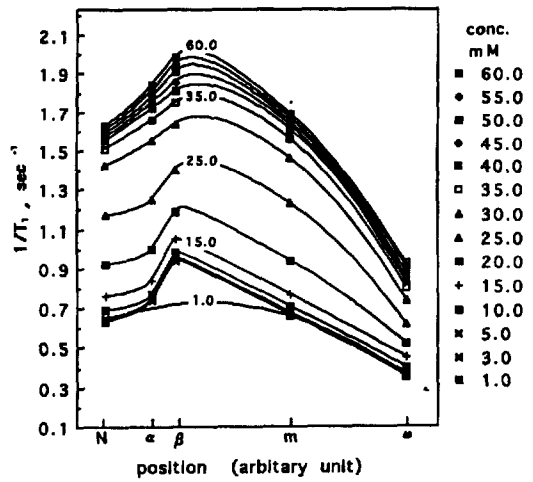

Figure 3. Plot of proton spin-lattice relaxation rate ($1/T_1$) of DTAB as a function of the ^{1}H-resonance of DTAB at a given concentration.

This results show that the value of $(1/T_1)_{intra}$ have the same tendency as the one of the chemical shifts difference $\Delta = \delta_{mic} - \delta_{mono}$ as mentioned above, *i.e.*, the β has the largest value, and becomes progresively small as the position of the proton atom reaches either polar head and chain end. This variation represent directly the degree of rotational correlation time and internal motion of each segment of surfactant molecule under the assumption of fully extend hydrocarbon chain.

In Figure 3, the relaxation rates of surfactant molecules were plotted as a function of the ^{1}H-position at each concentration. The scale of the axis of the ^{1}H-position is given from the assumption of the length of C-C bond being one (in arbitary unit) including C-N bond.

From Figures 2 and 3, a marked increase in the $1/T_1$ value with increasing the surfactant concentration above 1st. CMC (*i.e.*, spherical micelle region) is found in all protons. This behavior may be attributed to a severe immobilization at the polar head as well as at the hydrocarbon chain, because surfactant molecules interact strongly with neighboring molecules, counterions and water molecules at the micellar surface, and because the mobility of the hydrocarbon chain is greatly restricted due to the packing of the chains. Accordingly, the overall motion of the surfactant molecule becomes more and more restricted, implying that the internal motions become more important for the relaxation process. As for the terminal methyl, ω, it has a prominent segmental mobility, *i.e.*, it has the smallest value of $1/T_1$, irrespective of the surfactant concentration. It can be inferred that the micellar interior is likely to have properties of approaching to those of a liquid hydrocarbon environment, as already stated by others in the same system,[33,34] and the shorter chain systems.[36] Each segments of hydrocarbon chain except for α have the higher mobility as the position reaches the chain end, ω. And it has the good relation with the results of fluorescence and NMR measurements that when the hydrophobic materials like benzene, eosine and pyrene were dissolved in micellar solutions, their position in the micelle interior is near to β.[25,26]

Figure 3 clearly shows that the $1/T_1$ values of α is somewhat larger than those of the polar head, and somewhat smaller than those of β in all concentration. This variation can be interpreted as the effect of the water molecules penetrated into the micelle interior up to α-position. The environment formed by penetrating water molecules to this position can give somewhat higher mobility to α segment. Tanford[25] and Zielinski *et al.*,[32] found that the penetration of water molecules reaches to β position in case of OTAB[1] having eight carbon chain length, and this penetration effect reduced gradually with increasing carbon chain length. In spherical micelle region of Figure 3, the difference of $1/T_1$ values between α and polar head is about 0.1 sec^{-1}, and does not vary with concentration. But above the surfactant concentration of 32.0 mM, this difference is doubled such as 0.2 sec^{-1}, and this increasing tendency is continuously observed. This implies the reduction of water penetration above 32.0 mM. And this can be explained as a results of the deformation of spherical micelle to ellipsoidal one due to the shortening of the distance among polar heads. To confirm this, we applied the pseudophase model to the values of the relaxation rates.

The lifetime of a micelle is substantially shorter than the relaxation times being measured and the observed $1/T_1$ value is considered to be a weighted average of the rate for micelles and for monomers:

$$(1/T_1)_{obs} = \frac{CMC}{C_t} \cdot (1/T_1)_{mono} + \frac{C_t - CMC}{C_t} \cdot (1/T_1)_{mic}$$

where the notation used is the same as those of chemical shift. Since the monomer concentration above the 1st. CMC is nearly constant, the value of $(1/T_1)_{mono}$ in the micelle region is regared as constant. Then the $(1/T_1)_{mic}$ can be calculated for various concentrations. In Figure 4, the values of $(1T_1)_{mic}$ of each protons thus determined are plotted as as function of concentration. The slopes for all protons changed around 32.0 mM, and in each region, above and

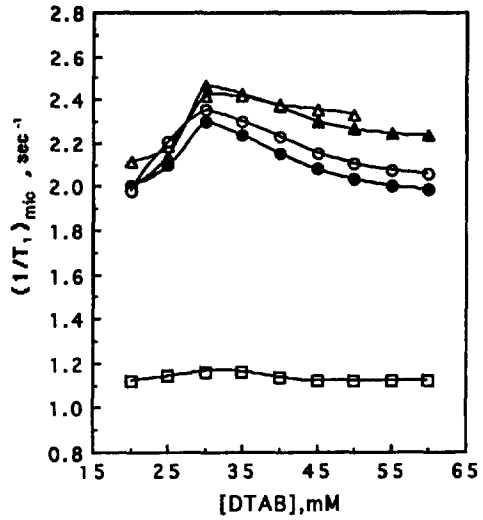

Figure 4. The relaxation rate of proton in micelle $\{(1/T_1)_{mic}\}$ as a function of the concentration of DTAB in spherical micelle region in water (D_2O). (● : *N*, ▲ : α, △ : β, ○ : *m*, □ : ω).

below this concentration, the slopes for each protons are similar except ω proton. Their values are $(-1.2\pm 0.4)\times 10^{-2}$ and $(3.6\pm 0.7)\times 10^{-2}$, respectively. The self-diffusion coefficients of the micelles are low enough, the intermicellar dipole-dipole interaction should be negligible. The slope change shown above must be explained by the internal motion of the hydrocarbon chains within the micelle. Also the high charge on micelles must ensure that close contact between micelles is unlikely, *i.e.*, the interactions between micelles are strongly repulsive.[8] Consequently the slope change of $(1/T_1)_{mic}$ to the concentration around 32.0 mM is attributed to the change in micellar structure. The value of $(1/T_1)_{mic}$ of ω is indifferent through all the concentration region *i.e.*, the mobility of the deepest micelle interior is not changed in changing of the micelle structure.

In summary,[37] the micellization process of DTAB in aqueous solution is as follows: (i) it exists as a single ion *i.e.*, monomer, by dissolving in water at low concentration, but the unstability of hydrocarbon chain leads a transition of forming spherical micelle at the 1st. CMC (16.0 mM), (ii) spherical micelle changes its shape to ellipsoidal one through the deformation within each micelles around 32.0 mM, (iii) downfield chemical shift on this micellization reflects the increased fraction of *trans* conformer, and (iv) the result of the spin-lattice relaxation rate shows the presence of motional gradient along hydrocarbon chain of DTAB molecules.

Acknowledgement. This work was supported by Seoul National University DAEWOO Research Fund (1990).

References

1. Abbreviations used: CMC, critical micelle concentration; DTAB, dodecyltrimethylammonium bromide; TTAC, tetradecyltrimethylammonium chloride; CTAB, cetyltrimethylammonium bromide; CTAC, cetyltrimethylammonium monium chloride; DDAC, dodecyldimethylammonium chloride; OTAB, octyltrimethylammonium bromide.
2. B. O. Persson, T. Drakenberg, and B. Lindman, *J. Phys. Chem.*, **80**, 2124 (1976).
3. E. Jungermann, "Cationic Surfactants", Dekker, New York (1970).
4. J. H. Fendler, "Membrane Mimetic Chemistry", Wiley, New York (1982).
5. M. T. Bashford and E. M. Woolley, *J. Phys. Chem.*, **89**, 3173 (1985).
6. M. N. Jones and J. Piercy, *Trans. Faraday Soc.*, **68**, 1839 (1972).
7. B. W. Barry and R. Wilson, *Colloid Polym. Sci.*, **256**, 251 (1978).
8. J. E. Brady, D. F. Evans, G. G. Warr, F. Grieser, and B. W. Ninham, *J. Phys. Chem.*, **90**, 1853 (1986).
9. M. R. Böhmer, L. K. Koopal, and J. Lyklema, *J. Phys. Chem.*, **95**, 9569 (1991).
10. M. L. Martin, G. J. Martin, and J. J. Delpuech, "Practical NMR Spectroscopy", Heyden, London (1980).
11. T. Drakenberg and B. Lindman, *J. Colloid Interface Sci.*, **44**, 184 (1973).
12. C. Chachaty, *Progress in NMR Spec.*, **19**, 183 (1987).
13. Y. Chevalier and C. Chachaty, *Colloid & Polymer Science*, **262**, 489 (1984).
14. L. Odberg, B. Svens, and I. Danielsson, *J. Colloid Interface Sci.*, **41**, 298 (1972).
15. J. Ulmius and H. Wennerstrom, *J. Magn. Resonance*, **28**, 309 (1977).
16. V. B. Cheney and D. M. Grant, *J. Amer. Chem. Soc.*, **89**, 5319 (1967).
17. J. Ulmius, B. Lindman, G. Lindblom, and T. Drankenberg, *J. Colloid Interface Sci.*, **65**, 88 (1978).
18. J. B. Rosenholm, T. Drakenberg, and B. Lindman, *J. Colloid Interface Sci.*, **63**, 538 (1978).
19. N. Muller and F. E. Platko, *J. Phys. Chem.*, **75**, 547 (1971).
20. J. H. Fendler, E. J. Fendler, R. T. Medary, and O. A. Elseoud, *J. Chem. Soc., Faraday Trans. 1*, **69**, 280 (1973).
21. B. O. Persson, T. Drakenberg, and B. Lindman, *J. Phys. Chem.*, **83**, 3011 (1979).
22. Z. Gao, R. E. Wasylishen, and J. C. T. Kwak, *J. Colloid Interface Sci.*, **137**, 137 (1990).
23. J. N. Israelachvili, D. J. Mitchell, and B. W. Ninham, *J. Chem. Soc., Faraday Trans. 2*, **72**, 1525 (1976).
24. P. J. Flory, "Statistical Mechanics of Chain Molecules", Wiley, New York (1969).
25. C. Tanford, "The Hydrophobic Effect: Formation of Micelles and Biological Membranes", 2nd Ed., Wiley, New York (1980).
26. R. Zana, *J. Colloid Interface Sci.*, **78**, 330 (1980).
27. O. Soderman, H. Walderhaug, U. Henriksson, and P. Stilbs, *J. Phys. Chem.*, **89**, 3693 (1985).
28. O. Soderman, U. Henriksson, and U. Olsson, *J. Phys. Chem.*, **91**, 116 (1987).
29. D. Stigter, *J. Colloid Interface Sci.*, **23**, 379 (1967).
30. D. J. Mitchell and B. W. Ninham, *J. Chem. Soc., Faraday Trans. 2*, **77**, 601 (1981).
31. H. Maeda, S. Ozeki, S. Ikeda, H. Okabayashi, and K. Matsushita, *J. Colloid Interface Sci.*, **76**, 532 (1980).
32. R. Zielinski, S. Ikeda, H. Nomura, and S. Kato, *J. Colloid Interface Sci.*, **129**, 175 (1989).
33. E. Williams, B. Sears, A. Allerhand, and E. H. Cordes, *J. Amer. Chem. Soc.*, **95**, 4871 (1973).

34. R. Zana, "Surfactant Solutions", Marcel Dekker, New York (1987).
35. Y. Uzu, Y. Saito, and M. Yokoi, *Bull. Chem. Soc. Jpn.*, **62**, 1370 (1989).
36. Z. Gao, J. C. T. Kwak, and R. E. Wasylishen, *J. Colloid Interface Sci.*, **126**, 371 (1988).
37. K. W. Woo, *SNU-DAEWOO Research Abstracts*, **4**, 105 (1992).

Purification and Characterization of *Bacillus Licheniformis* α-Amylase from Genetically Cloned *E. coli* NM522

Wol-Suk Cha* and Euy Kyung Yu†

Department of Chemical Engineering, Chosun University, Kwangju 501-759
†Department of Chemistry, Sejong University, Seoul 133-150
Received February 19, 1993

Bacillus licheniformis α-amylase cloned in *E. coli* genetically was purified by ammonium sulfate fractionations, DEAE-Sephacel, Mono-S, and Superose-6 column chromatographies. The highly purified α-amylase preparation showed 221.8 units per mg protein with 30% yield. Disc gel electrophoresis showed one major protein band. The molecular weight of *B. licheniformis* α-amylase produced in *E. coli* was 55,000 daltons by SDS gel electrophoresis. The K_m value of *Bacillus licheniformis* α-amylase produced in *E. coli* was 0.22% and the V_{max} of the enzyme was 0.6-0.7% min by Hofstee plot. The activity of enzyme showed maximum through wide range of pH, from pH 4 to pH 8 but slowly decreased with increasing pH values. The enzyme required Ca^{2+} for its activity. At pH 8.0, the enzyme had about 25% activity after 15 min incubation at 90℃ with 1 mM Ca^{2+}.

Introduction

The enzyme α-amylase (α Amy; 1,4-α-D-glucanohydrolase, EC 3.2.1.) is an endoamylase and catalyzes the cleavage of the α-1,4-glucosidic linkage between glucose molecules in starch, glycogen, and dextrins. α-Amylase produces first dextrins, which are subsequently cleaved to maltose, glucose and branched oligosaccharides.

The α-amylases are widely distrubured in plant and animal kingdoms and are important for the utilization of polysaccharide *in vivo*. The α-Amylases of different origins exhibit the same specificity, namely catalysis of hydrolysis and have similar enzymatic properties, Ca^{2+} requirements and optimum pHs.[1,2] Interest has been focused on their mode of secretion, regulation of synthesis, protein structure and industrial application. In recent years, the amylase genes of *B. coagulans*,[3] *B. amyloliquefaciens*,[4] *B. licheniformis*,[5] and *B. stearothermophilus*[6,7] have been expressed in either *B. subtilis* and *E. coli*.

Taka-amylase A (TAA), a fungal α-amylase produced by *Aspergillus oryzae* and isolated in high yield,[8] catalyzes the endoamylolytic degradation of starch. The physical and chemical properties of this enzyme (TAA) have been extensively studied,[9] and three-dimensional structure of TAA have been investigated by X-ray structure analysis at 3Å resolution using the multiple isomorphour replacement method.[10] As the complete amino acid sequence determination progressed,[11] molecular model of TAA was completely constructed by fitting skeletal models to the electron density results. The substrate maltotriose-soaked crystal structure of TAA showed a possible binding mode between substrate and enzyme. On the basis of the difference Fourier analysis and the model fitting study, glutamic acid (Glu230) and aspartic acid (Asp 297) which are located at the bottom of the cleft were concluded to be the catalytic residues serving as the general acid and base, respectively.[12-14]

In order to support this acid-base model of TAA as general mechanism of α-amylase, the amino acid sequences inferred from *B. stearothermophilus* and *B. licheniformis* α-amylase gene was compared with amino acid sequence of TAA and the result showed homolozy in three functional groups.[15,16] The *B. licheniformis* α-amylase is the liquefying enzyme most widely used in industry and is the only heat and pH stable α-amylase that is known to show substantial activity in alkaline range at high temperature. This enzyme is stable between pH 6 and pH 11 at 25℃ and its optimal temperature is 76℃ at pH 9.0. The α-amylase gene of *B. licheniformis* (ATCC 278110) has been cloned[17] and the nucleotide sequence of a DNA fragment of 1,948 base pairs cotaining entire *B. licheniformis* α-amylase was determined completely.[18]

In this study, *B. licheniformis* α-amylase was produced in *E. coli* and was purified to homogeneity. The kinetic parameters, pH-optimums and thermostabilities of the α-amylase were determined.

Materials and Methods

Materials

Protein marker was purchased from Dalton. DEAE-Sephacel, Mono-S, Superose-6 were purchased from Pharmacia-

*To whom correspondence should be addressed.